Research Article | Vol. 25, No. 10 | 15 May 2017 | OPTICS EXPRESS 11217

Optics EXPRESS

Low voltage 25Gbps silicon Mach-Zehnder modulator in the O-band

DIEGO PEREZ-GALACHO,[1,*] CHARLES BAUDOT,[2] TIFENN HIRTZLIN,[1] SONIA MESSAOUDÈNE,[2] NATHALIE VULLIET,[2] PAUL CROZAT,[1] FREDERIC BOEUF,[2] LAURENT VIVIEN,[1] AND DELPHINE MARRIS-MORINI[1]

[1] *Centre de Nanosciences et de Nanotechnologies, CNRS, Univ. Paris-Sud, Université Paris-Saclay, C2N-Orsay, 91405 Orsay cedex, France*

[2] *ST Microelectronics, 850 rue Jean Monnet 38920 Crolles, France*

[*] *diego.perez-galacho@u-psud.fr*

Abstract: In this work, a 25 Gb ps silicon push-pull Mach-Zehnder modulator operating in the O-Band (1260 nm - 1360 nm) of optical communications and fabricated on a 300 mm platform is presented. The measured modulation efficiency ($V_\pi L_\pi$) was comprised between 0.95 V cm and 1.15 V cm, which is comparable to the state-of-the-art modulators in the C-Band, that enabled its use with a driving voltage of 3.3 V_{pp}, compatible with BiCMOS technology. An extinction ratio of 5 dB and an on-chip insertion losses of 3.6 dB were then demonstrated at 25 Gb ps.

OCIS codes: (130.0250) Optoelectronics; (130.4110) Modulators; (200.4650) Optical interconnects.

References and links

1. B. Jalali and S. Fathpour, "Silicon photonics," J. Lightwave Technol. **24**, 4600–4615 (2006).
2. M. J. Paniccia, "A perfect marriage: optics and silicon," Optik & Photonik **6**, 34–38 (2011).
3. P. Dong, Y.-K. Chen, G.-H. Duan, and D. T. Neilson, "Silicon photonic devices and integrated circuits," Nanophotonics **3**, 215–228 (2014).
4. A. Shacham, K. Bergman, and L. P. Carloni, "Photonic networks-on-chip for future generations of chip multiprocessors," IEEE T. Comput. **57**, 1246–1260 (2008).
5. R. A. Soref and B. R. Bennett, "Electrooptical effects in silicon," IEEE J. Quantum Elec. **23**, 123–129 (1987).
6. A. Shakoor, K. Nozaki, E. Kuramochi, K. Nishiguchi, A. Shinya, and M. Notomi, "Compact 1d-silicon photonic crystal electro-optic modulator operating with ultra-low switching voltage and energy," Opt. Express **22**, 28623–28634 (2014).
7. T. Baba, S. Akiyama, M. Imai, N. Hirayama, H. Takahashi, Y. Noguchi, T. Horikawa, and T. Usuki, "50-gb/s ring-resonator-based silicon modulator," Opt. Express **21**, 11869–11876 (2013).
8. S. Meister, H. Rhee, A. Al-Saadi, B. A. Franke, S. Kupijai, C. Theiss, L. Zimmermann, B. Tillack, H. H. Richter, H. Tian, D. Stolarek, T. Schneider, U. Woggon, and H. J. Eichler, "Matching pin-junctions and optical modes enables fast and ultra-small silicon modulators," Opt. Express **21**, 16210–16221 (2013).
9. D. Perez-Galacho, A. Abraham, S. Olivier, L. Vivien, and D. Marris-Morini, "Silicon modulator based on interleaved capacitors in subwavelength grating waveguides," Proc. SPIE 9891, 989112 (2016)
10. A. Abraham, O. Dubray, S. Olivier, D. Marrls-Morini, S. Menezo, and L. Vivien, "Low-voltage and low-loss silicon modulator based on carrier accumulation using a vertical slot waveguide," in Proceedings of IEEE 12th International Conference on Group IV Photonics (GFP) (IEEE, 2015), pp. 118–119.
11. M. Douix, D. Marris-Morini, C. Baudot, S. Crémer, D. Rideau, D. Perez-Galacho, A. Souhaite, R. Blanc, E. Batail, N. Vulliet, L. Vivien, E. Cassan, and F. Boeuf, "Design of integrated capacitive modulators for 56gbps operation," in Proceedings of IEEE 13th International Conference on Group IV Photonics (GFP) (IEEE, 2016). pp. 5-7
12. M. Sodagar, A. H. Hosseinnia, P. Isautier, H. Moradinejad, S. Ralph, A. A. Eftekhar, and A. Adibi, "Compact, 15 gb/s electro-optic modulator through carrier accumulation in a hybrid si/sio 2/si microdisk," Opt. Express **23**, 28306–28315 (2015).
13. A. Shastri, C. Muzio, M. Webster, G. Jeans, P. Metz, S. Sunder, B. Chattin, B. Dama, and K. Shastri, "Ultra-low-power single - polarization qam-16 generation without dac using a cmos photonics based segmented modulator," J. Lightwave Technol. **33**, 1255–1260 (2015).
14. D. J. Thomson, H. Porte, B. Goll, D. Knoll, S. Lischke, F. Y. Gardes, Y. Hu, G. T. Reed, H. Zimmermann, and L. Zimmermann, "Silicon carrier depletion modulator with 10 gbit/s driver realized in high-performance photonic bicmos," Laser Photon. Rev. **8**, 180–187 (2014).
15. Z. Xuan, Y. Ma, Y. Liu, R. Ding, Y. Li, N. Ophir, A. E.-J. Lim, G.-Q. Lo, P. Magill, K. Bergman, T. Baehr-Jones, and M. Hochberg, "Silicon microring modulator for 40 gb/s nrz-ook metro networks in o-band," Opt. Express **22**,

#290651 https://doi.org/10.1364/OE.25.011217
Journal © 2017 Received 14 Mar 2017; revised 19 Apr 2017; accepted 24 Apr 2017; published 4 May 2017

Optics EXPRESS

28284–28291 (2014).
16. D. Marris-Morini, C. Baudot, J.-M. Fédéli, G. Rasigade, N. Vulliet, A. Souhaité, M. Ziebell, P. Rivallin, S. Olivier, P. Crozat, X. L. Roux, D. Bouville, S. Menezo, F. Bœuf, and L. Vivien, "Low loss 40 gbit/s silicon modulator based on interleaved junctions and fabricated on 300 mm soi wafers," Opt. Express **21**, 22471–22475 (2013).
17. J. Wang, L. Zhou, H. Zhu, R. Yang, Y. Zhou, L. Liu, T. Wang, and J. Chen, "Silicon high-speed binary phase-shift keying modulator with a single-drive push–pull high-speed traveling wave electrode," Photonics Research **3**, 58–62 (2015).
18. P. Dong, C. Xie, L. L. Buhl, Y.-K. Chen, J. H. Sinsky, and G. Raybon, "Silicon in-phase/quadrature modulator with on-chip optical equalizer," J. Lightwave Technol. **33**, 1191–1196 (2015).
19. Q. Li, R. Ding, Y. Liu, T. Baehr-Jones, M. Hochberg, and K. Bergman, "High-speed bpsk modulation in silicon," IEEE Photonic. Tech. L. **27**, 1329–1332 (2015).
20. "Physical layer specifications and management parameters for 40 gb/s and 100 gb/s operation over fiber optic cables," IEEE Standard for Ethernet.
21. M. Chagnon, M. Osman, M. Poulin, C. Latrasse, J.-F. Gagné, Y. Painchaud, C. Paquet, S. Lessard, and D. Plant, "Experimental study of 112 gb/s short reach transmission employing pam formats and sip intensity modulator at 1.3 μm," Opt. Express **22**, 21018–21036 (2014).
22. M. Streshinsky, R. Ding, Y. Liu, A. Novack, Y. Yang, Y. Ma, X. Tu, E. K. S. Chee, A. E.-J. Lim, P. G.-Q. Lo, T. Baehr-Jones, and M. Hochberg, "Low power 50 gb/s silicon traveling wave mach-zehnder modulator near 1300 nm," Opt. Express **21**, 30350–30357 (2013).
23. T. Ferroti, B. Blampey, C. Jany, H. Duprez, A. Chantre, F. Boeuf, C. Seassal, and B. Ben Bakir, "Co-integrated 1.3ÂŧÂţm hybrid III-V/silicon tunable laser and silicon Mach-Zehnder modulator operating at 25Gb/s," Opt. Express **24**, 30379–30401 (2016).
24. D. Pérez-Galacho, D. Marris-Morini, R. Stoffer, E. Cassan, C. Baudot, T. Korthorst, F. Boeuf, and L. Vivien, "Simplified modeling and optimization of silicon modulators based on free-carrier plasma dispersion effect," Opt. Express **24**, 26332–26337 (2016).
25. C. Baudot, A. Fincato, D. Fowler, D. Perez-Galacho, A. Souhaité, S. Messaoudène, R. Blanc, C. Richard, J. Planchot, C. De-Buttet, B. Orlando, F. Gays, C. Mezzomo, E. Bernard, D. Marris-Morini, L. Vivien, C. Kopp, and F. Boeuf, "Daphne silicon photonics technological platform for research and development on wdm applications," Proc. SPIE 9891, 98911D (2016).
26. D. Petousi, P. Rito, S. Lischke, D. Knoll, I. Garcia-Lopez, M. Kroh, R. Barth, C. Mai, A.-C. Ulusoy, A. Peczek, G. Winzer, K. Voigt, D. Kissinger, K. Petermann, and L. Zimmermann, "Monolithically integrated high-extinction-ratio mzm with a segmented driver in photonic bicmos," IEEE Photonic. Tech. L. **28**, 2866–2869 (2016).

1. Introduction

Driven by the development of next generations of fully integrated optical interconnects, silicon photonics has attracted a great attention in the recent years. Its intrinsic CMOS compatibility naturally enables its integration with microelectronics, placing it as the best suited technology for short range optical fiber communications [1–4]. A lot of work has been dedicated recently to develop high performance silicon modulators based on the Free-Carrier Plasma Dispersion (FCPD) effect [5], either based on carrier injection [6–8], carrier accumulation [9–13] or carrier depletion [14–19]. The vast majority of them have been designed for the C-Band of optical communications systems (1530 nm - 1570 nm), traditionally used for long-haul optical communications. However, current standard of short range optical fiber communications prefers to use the O-Band (1260 nm - 1360 nm) [20] in order to benefit of the zero dispersion point of standard SMF28 fibers. Few propositions of modulators operating in the O-Band have been reported in the literature [15, 21–23], but all of them exhibited modulation efficiencies of about 2.5 V cm.

In this paper we present a silicon modulator based on a symmetric Mach-Zehnder interferometer operating in the O-Band of optical communication systems. Even though the FCPD effect is weaker at wavelengths around 1.31 µm than at 1.55 µm, the presented modulator exhibits a modulation efficiency comparable to its state-of-the-art counterparts in the C-Band, with a $V_\pi L_\pi$ product between 0.95 V cm and 1.15 V cm. Furthermore, it was possible to demonstrate high speed operation at 25 Gb ps using a driving voltage as low as 3.3 V_{pp}, compatible with BiCMOS technology. The present paper is organized as follows: in section 2 the design of the modulator and the description of the different experimental set-up are presented. Section 3 is devoted to the static measurements, while the high speed measurements of the modulator are presented in section 4. Finally, the main conclusions drawn from this work are presented in section 5.

Optics EXPRESS

2. Modulator design and fabrication

The cross-section of the phase shifter is schematically shown in Fig. 1(a). It is based on a lateral PN junction embedded in a rib waveguide. It has been designed following the simplified modeling approach proposed in [24]. Thanks to this approach more than 2000 designs were evaluated and compared, enabling a full optimization of the phase shifter. Silicon thicknesses were fixed by fabrication technology, therefore the considered parameters for optimization were: waveguide width, doping concentrations and junction position. The waveguide width was 400 nm, its height 300 nm, the thin slab that gives electrical access to the junction had a height of 50 nm. The targeted doping concentrations in the PN junction were P = 5×10^{17} cm^{-3} and N = 1.4×10^{18} cm^{-3}. The offset between the junction plane and the center of the waveguide was 25 nm towards the n-doped region to optimize the overlap of the depletion region and the optical mode, therefore optimizing the modulation efficiency. In order to reduce the access resistance to the junction, doping concentrations in excess of 10^{19} cm^{-3} were used for both P++ and N++ regions. 1 mm long phase shifter was embedded in both arms of a symmetric Mach-Zehnder modulator (MZM). Coplanar traveling wave electrodes in GSGSG configuration were used to drive the phase shifters in push-pull configuration. Thermal heaters implemented by means of metallic resistors were included in each arm of the MZM to set the operating point of the MZM. These resistors consisted on a narrow metallic line on the first metalization level of the Back End Of Line (BEOL) placed on top of the waveguide. This metalization level is sufficiently far from the waveguide to avoid optical losses while being close enough to efficiently transfer heat. The modulators were fabricated using the 300 mm technological platform from STMicroelectronics [25]. A SEM image of the fabricated modulator waveguide is shown in Fig. 1(b).The same phase shifter was also included in a ring resonator with the objective of measuring accurately the modulation efficiency of the phase shifter.

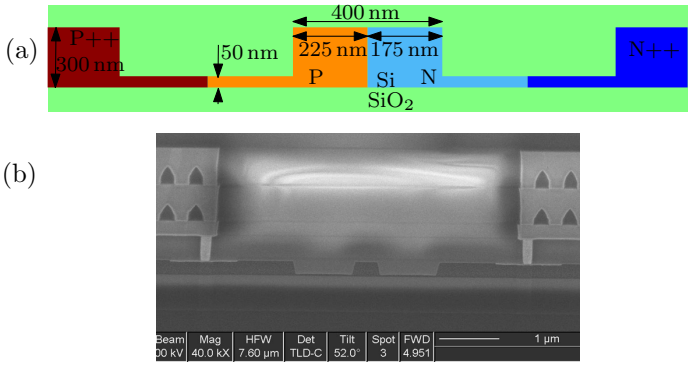

Fig. 1. Schematic view of the lateral PN junction based phase shifter.

The characterization of the modulators was performed for the TE-polarization, coupled in/out of the chip with grating couplers. Unless otherwise specified results are reported for a wavelength of 1310 nm, however the same results in terms of efficiency and high-speed operation were obtained in the whole O-Band. RF and DC electrical probes were used to electrically drive both PN diodes and heaters, respectively. The Yenista CT400 component tester was used to perform the static measurements. For the evaluation of the high-speed characteristics we used the setup depicted in Fig. 2 to record the small-signal electro-optical bandwidth and eye diagrams. The Agilent 86030A opto-RF vector network analyzer was used to measure the electro-optical bandwidth. For the eye diagram measurements, a pseudo random binary sequence (PRBS) generated by a Centellax TG1P4A source was amplified and added to the DC bias using a bias-tee. The optical output of the modulator was then coupled to a 32 GHz Agilent photodiode

Optics EXPRESS

connected to an Infiniium Agilent sampling oscilloscope. In both cases 50 Ω loads were applied on the other end of the traveling wave electrodes through DC blocks.

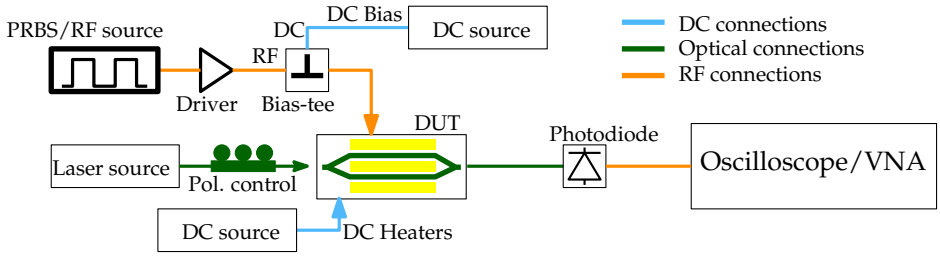

Fig. 2. Schematic view of the experimental setup employed to characterize the modulator.

3. Static measurements

The 1 mm long symmetric MZM and the ring resonator modulator were first measured in DC regime in order to extract the static performance of the modulator and the efficiency of the phase shifter. The normalized static optical transmission of the MZM and the ring resonator are shown in Fig. 3(a) and (b), respectively. A straight waveguide of similar length was used for the normalization. As the response of a symmetric MZM is independent with the wavelength, the transmission of the MZM was plotted as a function of the electrical power dissipated in the DC heater [Fig. 3(a)]. This allows a clear visualization of the shift of the transmission as a function of the voltage applied on the phase shifter. The excess on-chip insertion loss (IL) of the MZM was determined to be as low as 2.5 dB. From Fig. 3(a) a rough estimation of the modulation efficiency in the order of 1 V cm was obtained. In order to obtain an accurate measurement of the modulation efficiency, we used the transmission curves of the ring modulator [Fig. 3(b)] including the same phase shifter than the on in the MZM. Furthermore, the considered radius of 80 µm is large enough to avoid a difference in mode confinement into both phase shifters. Using the measured Free Spectral Range of the ring of 0.83 nm corresponding to group index of $n_g = 4.11$, the results of $V_\pi L_\pi$ product as a function of the applied voltage are reported in Fig. 3(c). It can be seen that the phase shifter exhibits a modulation efficiency values between 0.95 V cm and 1.15 V cm for a reverse applied voltage range from 1 V to 4 V. These values are the highest modulation efficiencies of carrier depletion based modulators in the O-Band.

Furthermore, in comparison with equivalent modulators in the C-Band, where the FCPD is stronger, the modulation efficiencies reported in this work are still among the state of the art results. Finally, the propagation loss of the active waveguide was estimated to be 1.5 $^{dB}/_{mm}$, this value was calculated first assuming that the propagation loss of the passive waveguide were 3 $^{dB}/_{cm}$. Then the measured value of $V_\pi L_\pi$ was used together with Electro-Optical simulations to deduce the corresponding excess propagation loss of 1.2 $^{dB}/_{mm}$. The IL of the 2x2 MMI couplers was then below 0.5 dB.

4. High-speed measurements

High-speed measurements were performed on the 1 mm long symmetric MZM. The measured small-signal electro-optical response as a function of the electric signal frequency is shown in Fig. 4. The heaters were used to ensure that the MZM is optically biased in the quadrature point for each measurement. A 3 dB electro-optical bandwidth of 18 GHz was obtained, meaning that the modulator is suitable to operate at the standard 25 Gb ps required for short range 100 GbE [20]. Electrical simulation were performed to obtain approximative values of the equivalent RC circuit of the modulators. Calculated values were: capacitance of $C = 0.64\,\mathrm{fF\,\mu m^{-1}}$ and resistance of

Optics EXPRESS

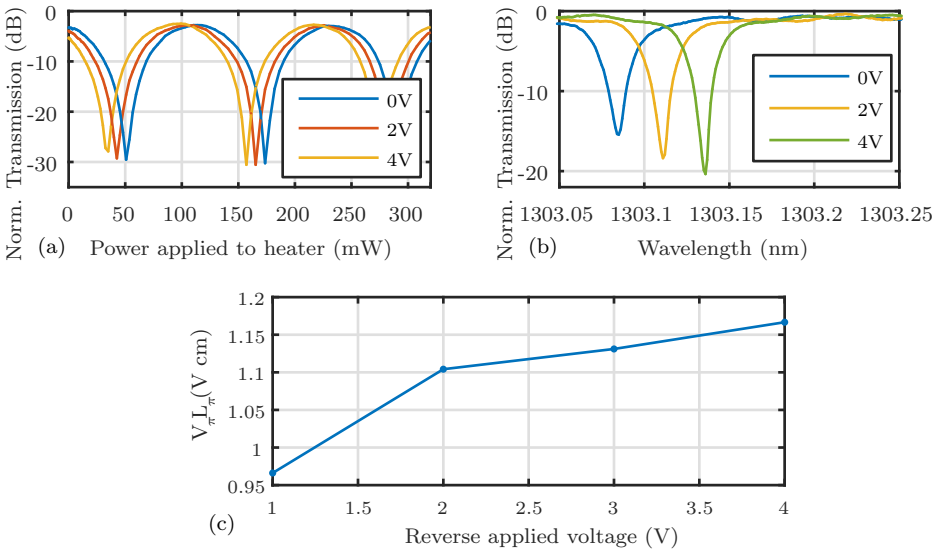

Fig. 3. Static response for several reverse applied voltages of (a) the 1 mm long symmetric MZM and (b) the ring resonator (b). (c) Measured modulation efficiency of the phase shifter as a function of the reverse applied voltage.

$R = 11.5\,\mathrm{k\Omega\,\mu m}$. This leads to an RC bandwidth limitation of 21 GHz, which is in agreement with the experimental data.

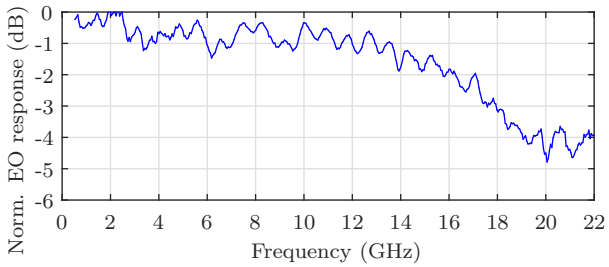

Fig. 4. Normalized small signal electro-optical response as a function of the applied frequency.

Data transmission at 25 Gb ps was then evaluated. Both arms of the 1 mm long MZM were driven in push-pull configuration, i.e. one arm is driven with the PRBS data signal and the other with its complementary. The heaters were used to set the interferometer in the quadrature point. It is worth mentioning that thanks to the low optical losses of the optical modulator, no optical amplification was required to perform the measurements. The applied voltage swing was 3.3 V_{pp}, with a DC bias of 1.7 V. This voltage swing is compatible with BiCMOS 0.25 µm technological node [26]. Using the driving voltages together with estimated capacitance we estimated a power consumption of 3.4 pJ bit^{-1}.The eye diagram at 25 Gb ps is reported in Fig. 5. An Extinction Ratio (ER) of 5 dB was obtained, while the additional losses due to high-speed modulation were only 1.1 dB (difference between high level of the eye and maximum static transmission level). This leads to a total on chip excess IL of 3.6 dB at this operating point.

A comparison of the performance with previously reported silicon modulators, including results in the C-Band, is shown in Table 1. It can be seen how the presented modulator outperforms

Optics EXPRESS

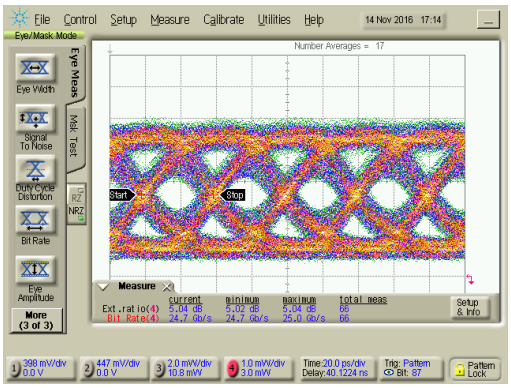

Fig. 5. Measured eye diagram at 25 Gb ps of the 1 mm long symmetric MZM with an applied voltage swing of 3.3 V_{pp} and 1.7 V DC bias.

the others in terms of efficiency while maintaining comparable performance in the rest of parameters.

Table 1. Comparison between silicon modulators.

	Band	$V_\pi L_\pi$	Loss	EO BW	Length	ER	V_{pp}
[14]	C-Band	2.3 V cm	13 dB	–	2 mm	8 dB	5.6 V_{pp}
[15]	O-Band	2.2 V cm	7 dB	30 GHz	47 μm (ring)	6.2 dB	4.8 V_{pp}
[16]	C-Band	2.4 V cm	4 dB	20 GHz	0.95 mm	7.9 dB	6 V_{pp}
[21]	O-Band	2.4 V cm	5 dB	20 GHz	6 mm	–	–
[22]	O-Band	2.43 V cm	7.1 dB	30 GHz	3 mm	3.4 dB	1.5 V_{pp}
[23]	O-Band	2.14 V cm	3.2 dB	28 GHz	2 mm	3.9 dB	2.5 V_{pp}
This work	O-Band	1.15 V cm	2.5 dB	18 GHz	1 mm	5 dB	3.3 V_{pp}

5. Conclusion

Optical communications in the O-Band have attracted a great attention in the optical interconnects community in order to exploit the zero dispersion point of conventional SMF28 optical fibers. However, the design of high performance silicon modulators with low driving voltages and shorter lengths in this band is challenging because the FCPD is weaker. In this work, we have presented a high performance push-pull silicon modulator based on a Mach-Zehnder interferometer operating in the O-Band. The performance of the modulator was comparable to the state-of-the-art modulators in the C-Band, where the FCPD is stronger. Moreover, thanks to its high modulation efficiency ($V_\pi L_\pi < 1.2$ V cm), the active length of the MZM was reduced to 1 mm maintaining at the same time a driving voltage compatible with BiCMOS technology.

Funding

European project Plat4m (FP7-2012-318178); European project Cosmicc (H2020-ICT-27-2015-688516); French Industry Ministry Nano2017 program.